Polymeric Surfactant P84/Polyoxometalate α-$PW_{12}O_{40}^{3-}$—A Model System to Investigate the Interplay between Chaotropic and Hydrophobic Effects

Philipp Schmid [1,2], Xaver Graß [1], Pratap Bahadur [3], Isabelle Grillo [4,†], Olivier Diat [2], Arno Pfitzner [1] and Pierre Bauduin [2,*]

[1] Institute of Inorganic Chemistry, University of Regensburg, Universitätsstraße 31, 93053 Regensburg, Germany; philipp.schmid@chemie.uni-regensburg.de (P.S.); xaver.grass@stud.uni-regensburg.de (X.G.); arno.pfitzner@chemie.uni-regensburg.de (A.P.)
[2] ICSM, Univ Montpellier, CEA, CNRS, ENSCM, Marcoule, France; olivier.diat@cea.fr
[3] Department of Chemistry, Veer Narmad South Gujarat University, Surat 395 007, India; pbahadur2002@yahoo.com
[4] Institut Laue-Langevin (ILL), 71 Avenue des Martyrs CS 20156, CEDEX 9, 38042 Grenoble, France; grillo@ill.fr
* Correspondence: pierre.bauduin@cea.fr
† In memory of Dr. Isabelle Grillo.

Supporting Information

Table of Contents

S1. Ternary phase diagram water/P84/HPW at room temperature 2
S2. Aggregation of P84 at 20 °C in absence and presence of HPW 3
S3. Further ^{1}H-NMR spectra of 2.5 wt% P84 in presence of HPW 6
S4. Fitting procedure of SANS and SAXS spectra at 50 °C 7
S4.1 Fundamentals 7
S4.2 Fitting 9
S5. References 15

S1. Ternary phase diagram water/P84/HPW at room temperature

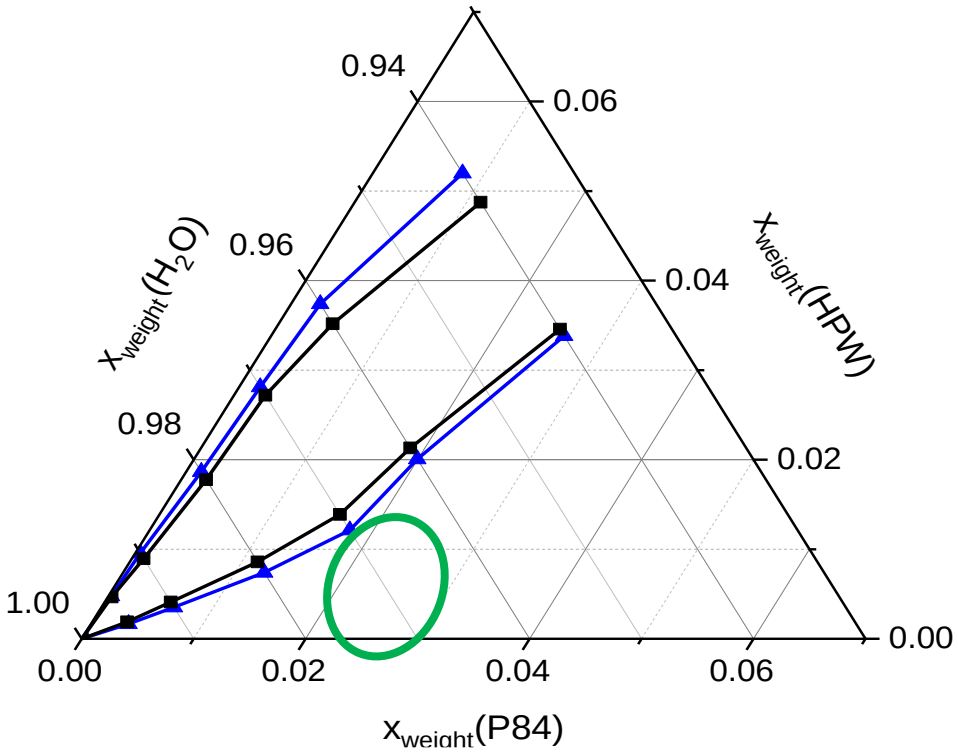

Figure S1. Partial ternary phase diagram water/P84/HPW provided in weight fraction (x_{weight}) at room temperature. The grey zone shows the biphasic region, whereas the blue area provides phases which appear blueish. The green ellipse indicates the area, in which it was worked in this contribution.

Figure S1 shows an excerpt the ternary phase diagram of water/P84/HPW at room temperature. The phase diagram is recorded in the water-rich corner of the diagram, *i.e.* c(water) ≥ *94 wt% = 0.94.* The diagram separates in three different regions: (*i*) transparent solution, (*ii*) blueish phases (blueish) and (*iii*) biphasic regions (grey). The occurrence of a biphasic region already hints on strong interactions between HPW and P84. Interestingly, only a small amount of P84 needs to be added to a HPW solution to reach a biphasic state, or blueish respectively. For example, 6 mmol kg^{-1} HPW are sufficient to lead to precipitation of 2.5 wt% P84 (~6 mmol kg^{-1}) which interestingly corresponds to a 1:1 stoichiometry, *i.e.* 1 HPW molecule and 1 P84 molecule lead to precipitation.
To guarantee monophasicity, our investigations focus on dilute HPW-P84 solutions, such as 2.5 wt% P84 in the presence of 2 mmol kg^{-1} HPW for scattering experiments or 2.5 wt% P84 up to 5.5 mmol kg^{-1} HPW in NMR experiments. This working area is marked with a green ellipse in Figure S1.

S2. Aggregation of P84 at 20 °C in absence and presence of HPW

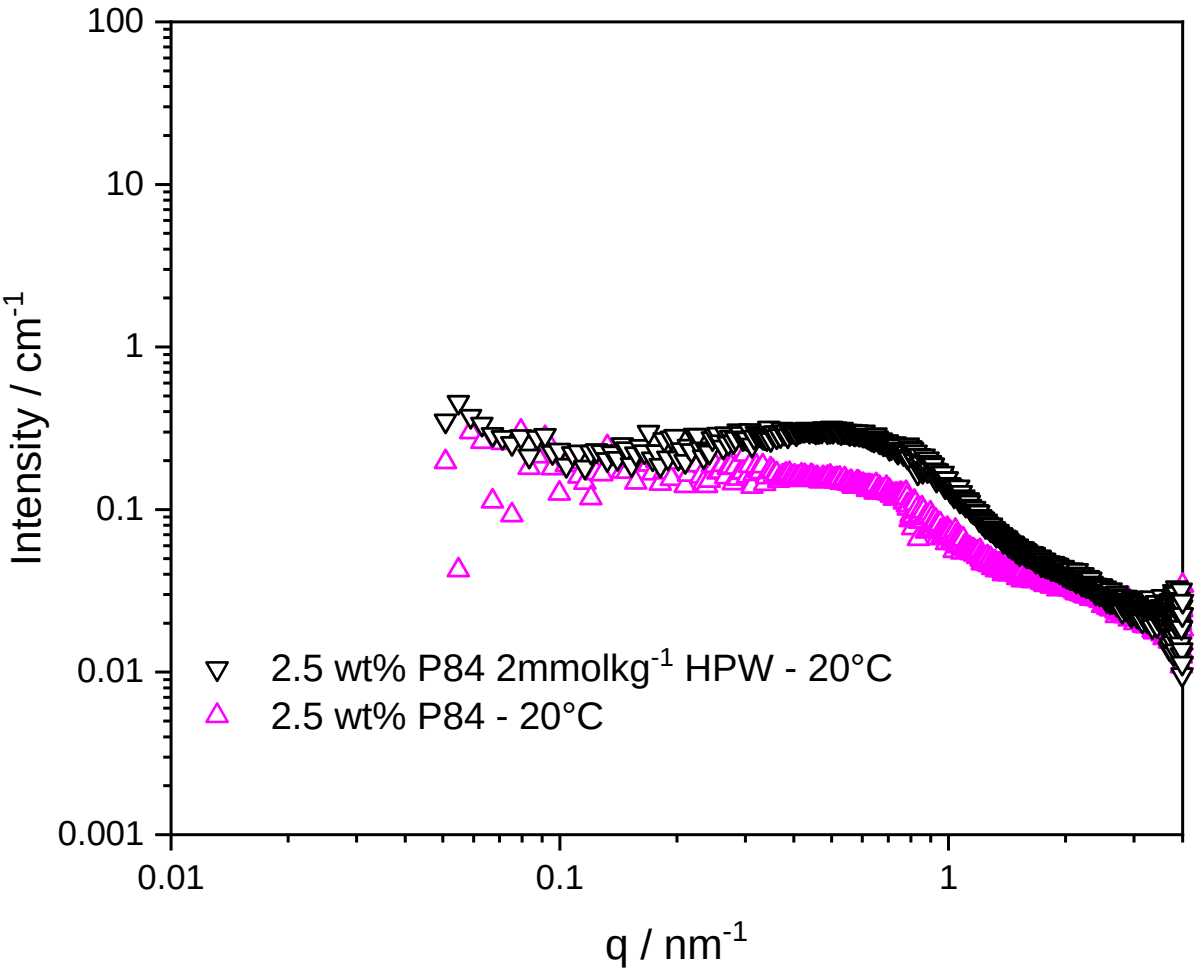

Figure S2. SANS spectra of 2.5 wt% P84 in D_2O at 20 °C. The spectra indicate that upon the addition of 2 mmol kg^{-1} HPW no significant aggregation of P84 takes place.

Figure S2 shows SANS spectra of 2.5 wt% P84 (in presence of 2 mmol kg^{-1} HPW) in D_2O. The SANS spectrum of 2.5 wt% P84 in D_2O shows a flat signal with a very slight correlation peak at 0.7 nm^{-1}. Upon the addition of 2 mmol kg^{-1} HPW the spectrum remains similar except of the enhanced correlation peak at 0.7 nm^{-1}. As a conclusion, the addition of HPW does not strongly affect the aggregation of P84 at 20 °C. It may be concluded by the absolute intensity of the correlation peak, that approximately two P84 molecules are coming together. A further interpretation of the SANS spectra cannot be drawn here.

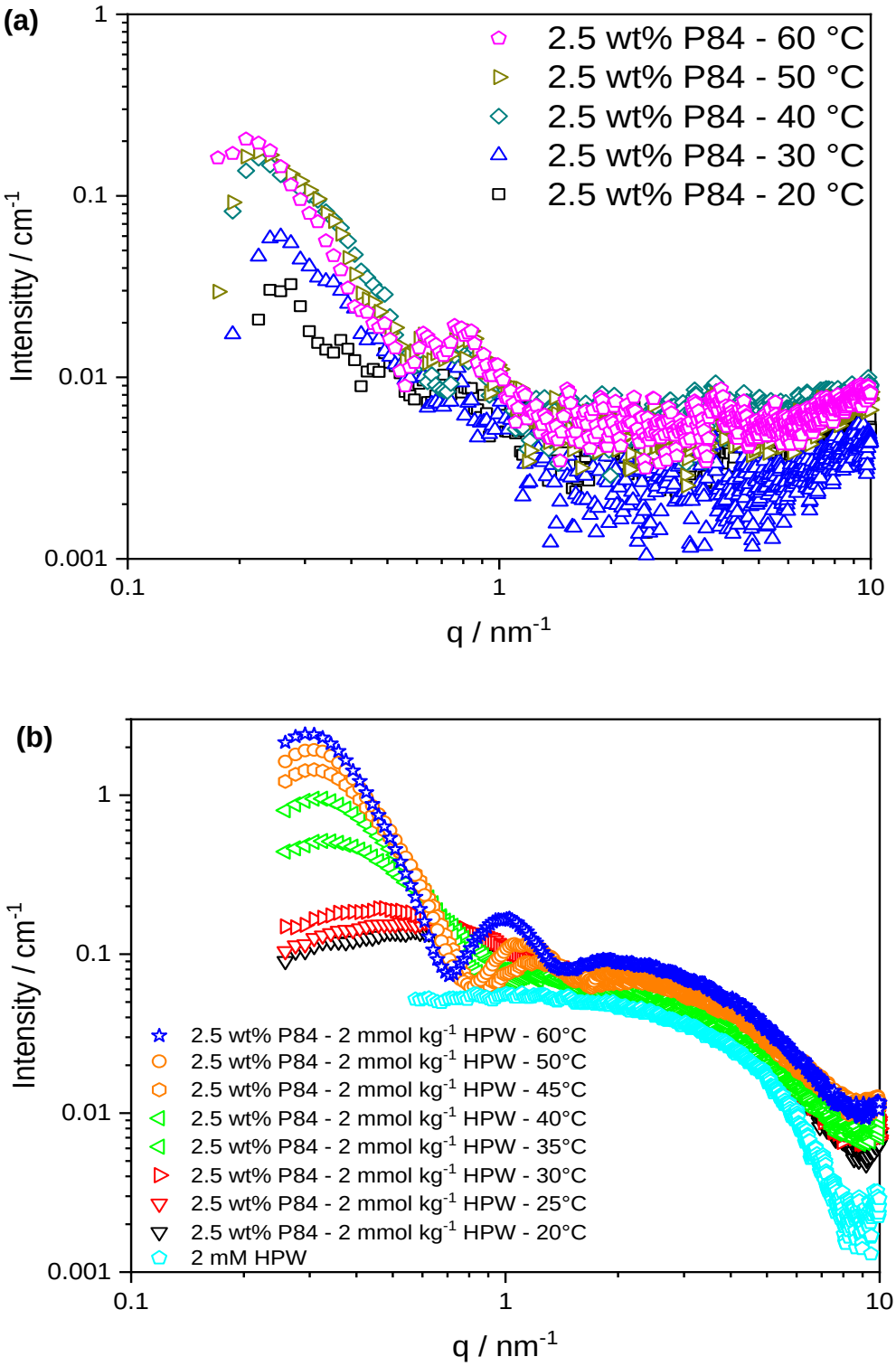

Figure S3. (a) SAXS spectra of 2.5 wt% P84 in water as a function of temperature between 20 and 60 °C. (b) SAXS spectra of 2.5 wt% P84 in presence of 2 mmol kg^{-1} HPW as a function of temperature between 20 and 60 °C. 2 mmol kg^{-1} HPW in water is given as a reference.

Figure S3a shows the evolution of the SAXS spectrum of 2.5 wt% P84 as a function of temperature (between 20 and 60 °C). The spectrum evolves from a nearly flat signal (20 °C, dark rectangles) to a signal typical for a spherical (core-shell) scatterer at higher temperatures. Such (core-shell) spectra can be attributed to the P84 micelle, where the PPO part represents the core and PEO the shell of the scatterer.

Figure S3b shows the SAXS spectra of 2.5 wt% P84 in presence of 2 mmol kg^{-1} HPW as a function of temperature between 20 and 60 °C. 2 mmol kg^{-1} HPW in water is given as a reference. Interestingly, the signal of 2 mmol kg^{-1} HPW changes already upon the addition of 2.5 wt% P84 at 20 °C, which indicates a strong interaction between HPW and unimeric P84 at 20 °C. A correlation peak arises at 0.7 nm^{-1} which corresponds to the correlation peak obtained in the SANS spectrum. A precise description of these assemblies (At 20 °C) is out of scope here and would require further SAXS and SANS experiments, *e.g.* variation of the P84 or HPW concentration. Consequently, no further conclusions are drawn on these aggregates.

Upon heating the sample, the SAXS spectrum drastically changes again, as a core-shell signal appears. This can be deduced to crossing the CMT. The evolution of the SAXS spectra upon heating indicates, that micelles are continuously formed.

An easy way, to determine the CMT of 2.5 wt% P84 in presence of 2 mmol kg^{-1} HPW is to plot the scattered intensity at q = 0.3 nm^{-1} versus the measured temperature, see Figure S4. Moreover, the count rate of 2.5 wt% P84 obtained by light scattering is plotted versus temperature (black squares). The plot of the scattered SAXS intensity at q = 0.3 nm^{-1} versus temperature (green squares) shows a kink at around 30 °C. This kink can be attributed to the CMT. Interestingly, the CMT is not affected upon the addition of HPW as it is in both cases in the red marked region, around 28 °C.

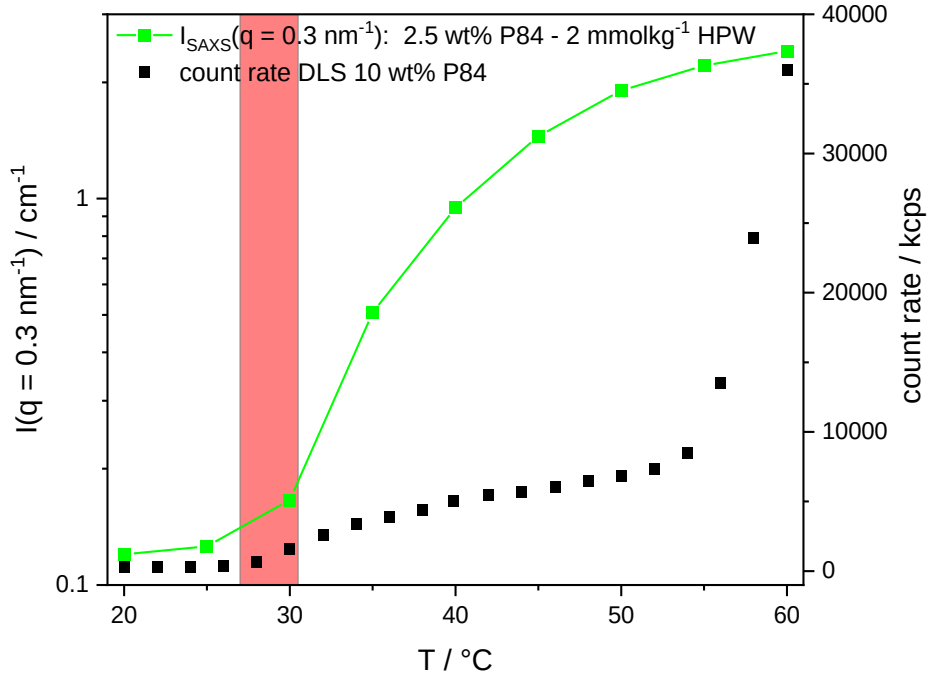

Figure S4. Count rate of 2.5 wt% P84 obtained by light scattering as a function of temperature (dark rectangles). In the manuscript the kink at 28 °C was attributed to the CMT, *i.e.* the critical micellization temperature. The intensity of 2.5 wt% P84 in presence of 2 mmol kg^{-1} HPW obtained by SAXS at q = 0.3 nm^{-1} (green data). The kink indicates again the CMT. The red region shows that the CMT is in a similar region in absence and presence of 2 mmol kg^{-1} HPW and significantly the POM does not influence the CMT of P84.

S3. Further ^{1}H-NMR spectra of 2.5 wt% P84 in presence of HPW

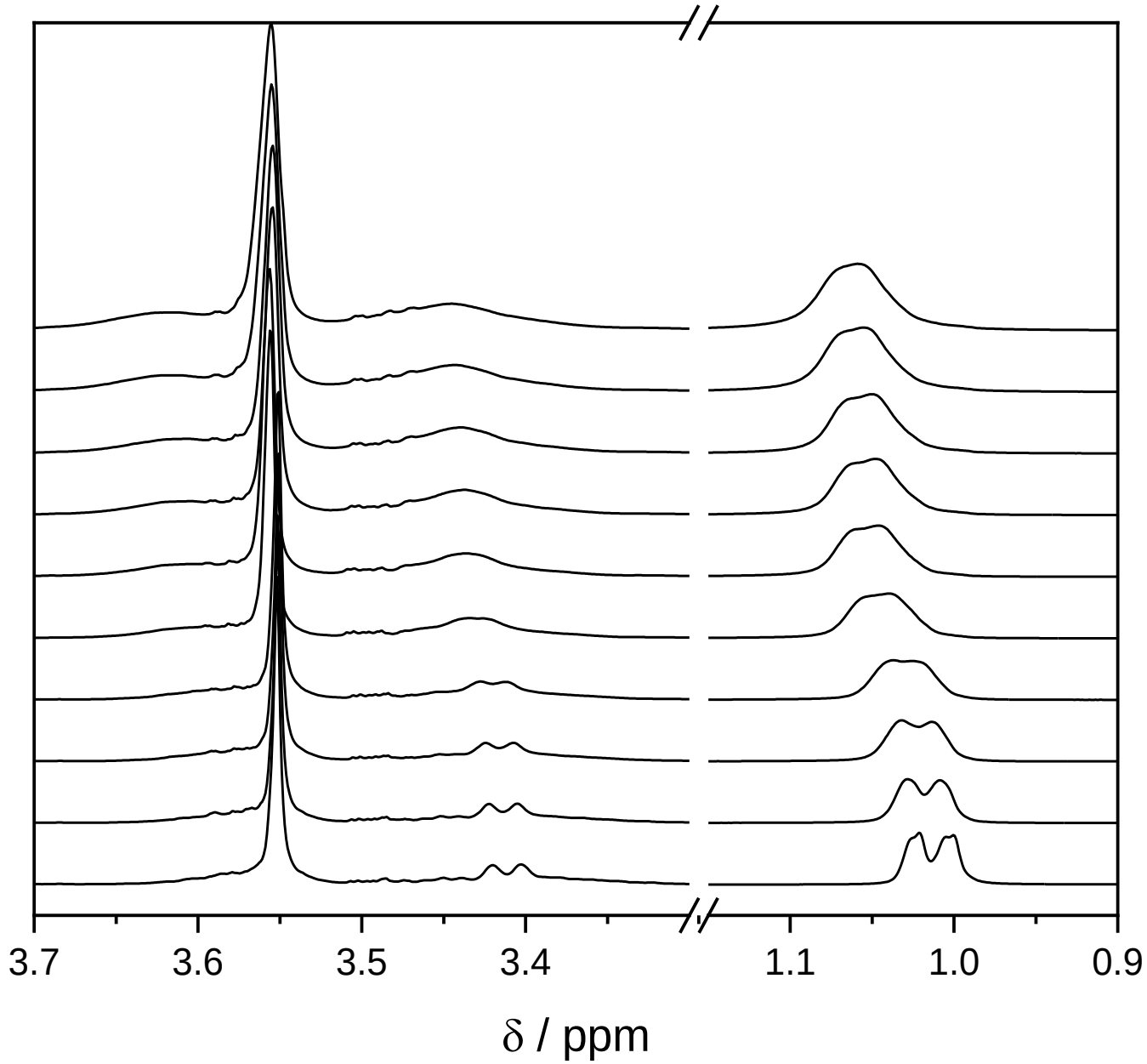

Figure S5. ^{1}H-NMR spectra of 2.5 wt% P84 at 20 °C in D_2O in presence of 0, 0.46, 0.99, 1.70, 2.70, 3.46, 3.94, 4.41, 5.02, 5.50 mmol kg^{-1} HPW (bottom to top). The presence of HPW causes a strong shift of signals stemming from the PPO, whereas the PEO signal remains untouched.

Figure S5 shows further NMR spectra of 2.5 wt% P84 in D_2O with a variable amount of HPW. The concentrations of HPW are given in the description of Figure S5. The general trend persists, that only signals stemming from the PPO part of P84 are affected upon the addition of HPW. The position of the singlet signal of PEO remains unchanged.

S4. Fitting procedure of SANS and SAXS spectra at 50 °C

S4.1 Fundamentals

Introduction

In this contribution, the focus is on micellar aggregates of P84, which are present at 50 °C. Consequently, the SAXS (and SANS) spectra are only fitted in the low q-regime, *i.e.* $q < 2$ nm^{-1} to exclude the pure POM contribution, which typically arise at $q > 3$ nm^{-1} (in SAXS).[1]

All SAXS- and SANS-fits were performed using the SASView version 5.0.3,[2] where the scattered intensity, *I(q)*, of an isotropic sample containing identical and randomly oriented particles is expressed by Eq. S1.

$$I(q) = n * V^2 * \Delta\rho^2 * P(q) * S(q) \quad \textbf{(S1)}$$

with n the number density of the scattering object, V its volume, the scattering contrast $\Delta\rho = \rho_{particle} - \rho_{solvent}$, the form factor $P(q)$ and the structure factor $S(q)$. The form factor $P(q)$ describes the shape of the scattering object, while the structure factor $S(q)$ describes the higher order arrangement of the scattering objects.

Determination of electron densities

In order to determine the scattering contrast in SAXS, the individual electronic densities $\rho_{particle}$ and $\rho_{solvent}$ were calculated by Eq. S2.

$$\rho_i = \frac{\sum_j b_j}{v_i} * l_{Thomson} \quad \textbf{(S2)}$$

With b_j being the number of electrons in the jth atom, v_i the scattering objects volume and $l_{Thomson}$ the Thomson length ($l_{Thomson}$ = 2.82 × 10^{-13} m). Table S1 shows literature ρ-values for the investigated compounds.

Table S1. (Reported) scattering length densities in SAXS and SANS of the investigated compounds. Note, that in case of ρ(P84) the pure PO and EO moiety is taken into account, *i.e.* hydration water is neglected, while it is known that hydration water increases the scattering length density.[3]

Compound	ρ^{SAXS} / 10^{10} cm^{-2}	ρ^{SANS} / 10^{10} cm^{-2}
$PW_{12}O_{40}^{3-}$	74.9[1]	5.9[2]
H_2O	9.4	-
D_2O	-	6.4
Pluronic® surfactant (P84)	PEO: 10.9[3]	PEO: 0.3[3]
	PPO: 9.6[3]	PPO: 0.7[3]

[1] taken from Naskar *et al.*[4]
[2] taken from Schmid *et al.*[5]
[3] taken from Grillo *et al.*[3]

It is worth mentioning, that via

$$\rho_{PO,\ hydrated}^{SAXS/SANS} = \Phi_{PO}\rho_{PO}^{SAXS/SANS} + \Phi_{H_2O/D_2O}\rho_{H_2O/D_2O}^{SAXS/SANS} \quad \textbf{(S3)}$$

$$\rho_{EO,\ hydrated}^{SAXS/SANS} = \Phi_{EO}\rho_{EO}^{SAXS/SANS} + \Phi_{H_2O/D_2O}\rho_{H_2O/D_2O}^{SAXS/SANS} \quad \textbf{(S4)}$$

the experimental scattering length densities of P84 are higher/lower compared to the pure ρ(PO) and ρ(EO) respectively, which was observed nicely for other polymeric surfactants such as F127.[3]

P84 micelle dimension in literature

Furthermore, Table S2 shows literature data in the dimension on P84 micelles, *i.e.* the micelle core radius (PPO) and the shell (EO) thickness in order to get a first estimation of the micelle size. Note, that these data are reported for an aqueous P84 solution with c(P84) = 5 wt%, *i.e.* the doubled concentration as in our contribution. Consequently, these values can only be used as a first guidance.

Table S2. Dimension (in nm) of a spherical P84 micelle at c(P84) = 5 wt%.[6]

$r_{PPO\text{-}core}$	$r_{PEO\text{-}shell}$	$r_{hard\text{-}sphere}$
4.0	3.0	7.0

S4.2 Fitting

Fitting of 2.5 wt% P84 in water (D_2O or H_2O)

As a first step, the SANS spectrum of 2.5 wt% P84 at 50 °C is fitted. In order to take into account the micelle-micelle interactions, a hard sphere structure factor is applied, represented by the hard-sphere radius r_{HS}.
Table S3 shows the fitting parameters of the SANS spectrum of 2.5 wt% P84 in D_2O (2.5 wt% corresponds to a volume fraction of approximately 0.035). The parameters marked in green were fixed for obvious reasons as the $\rho_{solvent}$ is known (D_2O used as solvent) and the volume fraction of P84 can be calculated by the initial concentration of P84. The parameter "scale" is set to 1 which is due to the fitting procedure in SASView: As soon, as a *S(q)* contribution is introduced in the fit, the scale is set to 1 and the concentration of the scattering object, is represented by the volume fraction. The other parameters were fitted and gave reasonable values which are in general agreement with literature, as mentioned in the manuscript. Moreover, a polydispersity index (PDI) of PDI=0.2 was applied.

Table S3. Fitting parameters of 2.5 wt% P84 - SANS - Hard sphere S(q).

scale	1
background	0.02208
core-radius / nm	4.1
shell-thickness / nm	2.4
ϱ_{core} / 10^{10} cm^{-2}	1.4
ϱ_{shell} / 10^{10} cm^{-2}	5.55
$\varrho_{solvent}$ / 10^{10} cm^{-2}	6.4
volume fraction	0.035[4]
r_{HS} / nm	6.5

[4] calculated from Jain *et al.*[6]

As the micelle dimensions (core-radius (PPO) and shell thickness(PEO)) are in well agreement with the data reported [6] the applied fit can be considered to lead to reasonable and robust data. This is further supported, as the fitted scattering length densities are in a reasonable region for (partially) hydrated polymeric surfactant micelles, *cf.* equations S3 and S4 and Grillo *et al.*[3]

In a next step, the corresponding SAXS spectrum (2.5 wt% P84 at 50 °C) is similarly fitted and fitting parameters are shown in Table S4.

Table S4. Fitting parameters of 2.5 wt% P84 - SAXS - Hard sphere S(q).

scale	1
background	0.006424
radius / nm	4.1
thickness / nm	2.4
ϱ_{core} / 10^{10} cm^{-2}	9.47
ϱ_{shell} / 10^{10} cm^{-2}	9.76
$\varrho_{solvent}$ / 10^{10} cm^{-2}	9.4
volume fraction	0.035[4]

r_{HS} / nm	4.3

[4] calculated from Jain *et al.*[6]

Table S4 depicts the fitting parameters of the SAXS spectrum of 2.5 wt% P84 in H_2O at 50 °C. The green marked parameters were fixed. The values for the radius (micelle core) and the shell thickness (micelle corona) were taken from the SANS fit (marked in yellow), *cf.* Table S3, in order to provide self-consistency of the fitting procedure. The other parameters were fitted and lead to physically reasonable values. By doing this self-consistent SANS/SAXS fits and their good results in comparison with literature, the fit procedure can be considered to lead to robust and reliable results.

Fitting of 2.5 wt% P84 - 2 mmol kg^{-1} HPW in water (D_2O or H_2O)

Upon the addition of 2 mmol kg^{-1} HPW both, the SANS and the SAXS spectrum of 2.5 wt% P84 showed a strong decrease in the low *q*-part. This was explained by repulsive forces between the P84 micelles upon the adsorption of the anionic PW onto the P84 micelles. In order to manifest those repulsive interactions a Hayter-MSA[7][8] *S(q)* contribution was applied in the following fits, *i.e.* 2.5 wt% P84 in presence of 2 mmol kg^{-1} HPW at 50 °C.

Table S5. Fitting parameters of 2.5 wt% P84 – 2 mmol kg^{-1} HPW - SANS - Hayter-MSA S(q).

scale	1
background	0.013537
radius / nm	3.6
thickness / nm	1.9
ϱ_{core} / 10^{10} cm^{-2}	1.4
ϱ_{shell} / 10^{10} cm^{-2}	5.55
$\varrho_{solvent}$ / 10^{10} cm^{-2}	6.4
volume fraction	0.035[4]
charge / e$^-$	47
temperature / K	328
ionic strength	0.0014
dielectricity	71
$r_{effective}$ / nm	5.6

[4] calculated from Jain *et al.*[6]

Table S5 provides the fitting parameters of the SANS spectrum of 2.5 wt% P84 in presence of 2 mmol kg^{-1} HPW in D_2O. The green marked parameters were fixed. Scale, $\varrho_{solvent}$, volume fraction, temperature and dielectricity were fixed by the measurement conditions. ϱ_{core} and ϱ_{shell} were used from the SANS fit of 2.5 wt% P84. As HPW is "invisible" in SANS it can be assumed (in rough estimation) that the scattering length densities of the PPO and the PEO part remain the same in presence of HPW. The other parameters were fitted. Interestingly, the micelle size shrinks, as both, the micellar core and shell decrease in size.

Table S6 shows the fitting parameters of the SAXS spectrum of 2.5 wt% P84 in presence of 2 mmol kg^{-1} HPW in H_2O. The green marked parameters were fixed, as they are fixed by the measurement conditions. The ϱ_{core} was taken from the SAXS fit of 2.5 wt% P84 in water, *cf.* Table S4. In order to justify the high contrast of HPW in SAXS, the ϱ_{shell} was a fitting parameter here. The parameters

marked in yellow, were taken from the SANS fit of 2.5 wt% P84 in presence of 2 mmol kg^{-1} HPW in D_2O, *cf.* Table S5, as they need to be the same independently from the method, *i.e.* SANS or SAXS. Interestingly, the fit reveals, that the core size shrinks drastically, whereas the micelle shell size is increased. This can only be explained by the partial penetration of the PW anion into the PPO core. Note, that the penetration of HPW into the PPO core is further evaluated in the next subchapter. The ϱ_{shell} is strongly increased which can be explained by the location of HPW in the micelle corona. The volume fraction is very small which is reasonable, as HPW (main contributor to scattering) is present in a volume fraction of 0.0006 (calculated by the molecular volume of PW [1]).

Table S6. Fitting parameters of 2.5 wt% P84-2 mmol kg^{-1} HPW - SAXS - Hayter-MSA S(q).

scale	1
background	0.065
radius / nm	2.2
thickness / nm	2.9
ϱ_{core} / 10^{10} cm^{-2}	9.47
ϱ_{shell} / 10^{10} cm^{-2}	18.7
$\varrho_{solvent}$ / 10^{10} cm^{-2}	9.4
volume fraction	0.00063[5]
charge / e^-	47
temperature / K	328
ionic strength	0.0014
dielectricity	71
$r_{effective}$ / nm	1.4

[5] calculated from the POM radius (r_{POM} ≈ 0.5 nm) given by Buchecker *et al.*[1]

Note, that the SAXS perfectly describes the experimental data, which shows the self-consistency of the SAXS/SANS fit procedure, especially as the charge and ionic strength were used from the SANS fit results for fitting the SAXS spectrum.

Location of the PW anion in the P84 micelle

Above and in the manuscript, we stated that the PW anions are located in the P84 micelle corona, but also partially penetrate the PPO core. As SAXS mainly investigates the scattering of the PW anion, *cf.* Table S1, we can clearly conclude on the PW location in the P84 micelle. Therefore, we assume five different scenarios:

(i) PW exclusively in the P84 corona (PEO).
(ii) PW exclusively in the P84 core (PPO).
(iii) PW homogeneously distributed over the micelle.
(iv) PW mostly in the P84 PPO core and partial entering of the PEO corona.
(v) PW mostly in the P84 PEO corona and partial entering of the PPO core.

To solve the question: "Where is the POM located in a P84 micelle?" again different fits of the SAXS spectrum 2.5 wt% P84 - 2 mmol kg^{-1} HPW at 50 °C are performed. To do this, we applied following procedure for the different scenarios (i) - (v).
(i): The core size and the shell thickness are fixed by the values obtained from the SANS fit, *cf.* Table S3. The location of the POM is adjusted by fixing ϱ_{core} to $9.47 \cdot 10^{10}$ cm^{-2}, while ϱ_{shell} is fitted with a

reasonable value of $20 \cdot 10^{10}$ cm^{-2} (due to high scattering length density of PW). Other parameters were fixed input parameters (either obtained from the SANS fit: charge or they were fixed by the experiment: volume fraction, temperature, ionic strength, dielectricity). The effective radius, $r_{effective}$ was fitted.
(ii): The core size and the shell thickness are fixed by the values obtained from the SANS fit, *cf.* Table S3. The location of the POM is adjusted by fixing ϱ_{shell} to $9.75 \cdot 10^{10}$ cm^{-2}, while ϱ_{core} is fitted with a reasonable value of $23 \cdot 10^{10}$ cm^{-2} (due to high scattering length density of PW). Other parameters were fixed input parameters (either obtained from the SANS fit: charge or they were fixed by the experiment: volume fraction, temperature, ionic strength, dielectricity). The effective radius, $r_{effective}$ was fitted.
(iii): Several parameters were fixed input parameters (either obtained from the SANS fit: charge or they were fixed by the experiment: volume fraction, temperature, ionic strength, dielectricity). The effective radius, $r_{effective}$ was fitted. Moreover, the radius of the homogeneous sphere (r_{total}) and its charge density (ϱ_{total}) were fitted within physical meaning.
(iv): Several parameters were fixed input parameters (either obtained from the SANS fit: charge or they were fixed by the experiment: volume fraction, temperature, ionic strength, dielectricity). The effective radius, $r_{effective}$ was fitted. Furthermore, the dimension of the micelle (r_{core} and shell thickness) and the scattering length density ϱ_{core} (ϱ_{shell} was fixed by SAXS measurement in absence of HPW) were fitted within physical meaning.
(v): Several parameters were fixed input parameters (either obtained from the SANS fit: charge or they were fixed by the experiment: volume fraction, temperature, ionic strength, dielectricity). The effective radius, $r_{effective}$ was fitted. Furthermore, the dimension of the micelle (r_{core} and shell thickness) and the scattering length densities ϱ_{shell} (ϱ_{core} was fixed by SAXS measurement in absence of HPW) were fitted within physical meaning.

Table S7 summarized the fitting parameters of the five different scenarios, while Figure S6 provides a plot of the experimental data and the different fits.

Table S7. In- and output fitting parameters of the different fit procedures (i) - (v). The parameters (i) - (iv) do not lead to satisfying fits (indicated by the red background colour), whereas parameters in (v) produce a fit, which perfectly describes the measured spectrum (indicated with green background colour), *cf.* Figure S6.

	(i)	(ii)	(iii)	(iv)	(v)
scale	1	1	1	1	1
background	0.065	0.065	0.065	0.065	0.065
radius / nm	36	36	49 (r_{total})	40	22
thickness / nm	19.446	19.446		12	29
ϱ_{core} / 10^{10} cm^{-2}	9.47	23		24.294	9.47
ϱ_{shell} / 10^{10} cm^{-2}	20	9.75	19 (ϱ_{total})	9.75	18.7
$\varrho_{solvent}$ / 10^{10} cm^{-2}	9.4	9.4	9.4	9.4	9.4
volume fraction	0.00063	0.00063	0.00063	0.00063	0.00063
charge / e$^-$	47	47	47	47	47
temperature / K	328	328	328	328	328
ionic strength	0.0014	0.0014	0.0014	0.0014	0.0014
dielectricity	71.08	71.08	71.08	71.08	71.08

$r_{effective}$ / nm	12.411	13.141	49	14	12.512

The data from Table S7 in combination with Figure S6 (showing the goodness of the fits (i) – (v)) lead to the conclusion, that PW anions are in the PEO corona but enter partially the PPO core.

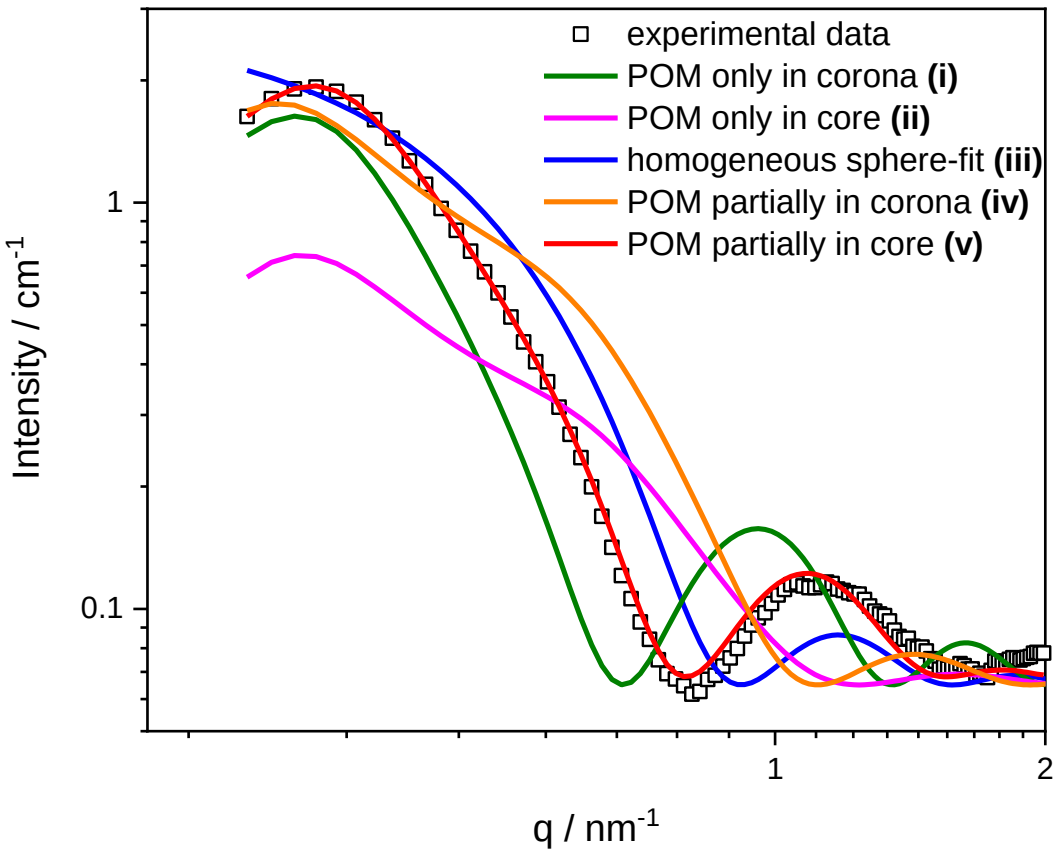

Figure S6. Fits obtained with the fitting parameters in Table S7. While fits (i) - (iv) do not lead to proper fitting results of the experimental data, fit (v) (POM in PEO corona, penetrating the PPO core) leads to a perfect fit of the experimental data.

S5. References

[1] T. Buchecker, P. Schmid, S. Renaudineau, O. Diat, A. Proust, A. Pfitzner, P. Bauduin, Polyoxometalates in the Hofmeister series, Chem. Commun. 54 (2018) 1833–1836. https://doi.org/10.1039/c7cc09113c.

[2] M. Doucet, J.H. Cho, G. Alina, Z. Attala, J. Bakker, W. Bouwman, P. Butler, K. Campbell, T. Cooper-Benun, C. Durniak, L. Forster, M. Gonzales, R. Heenan, A. Jackson, S. King, P. Kienzle, J. Krzywon, T. Nielsen, L. O'Driscoll, W. Potrzebowski, S. Prescott, R. Ferraz Leal, P. Rozycko, T. Snow, A. Washington, SasView version 5.0.3, (2020). https://doi.org/http://doi.org/10.5281/zenodo.3930098.

[3] I. Grillo, I. Morfin, S. Prévost, Structural Characterization of Pluronic Micelles Swollen with Perfume Molecules, Langmuir. 34 (2018) 13395–13408. https://doi.org/10.1021/acs.langmuir.8b03050.

[4] B. Naskar, O. Diat, V. Nardello-Rataj, P. Bauduin, Nanometer-Size Polyoxometalate Anions Adsorb Strongly on Neutral Soft Surfaces, J. Phys. Chem. C. 119 (2015) 20985–20992. https://doi.org/10.1021/acs.jpcc.5b06273.

[5] P. Schmid, T. Buchecker, A. Khoshsima, D. Touraud, O. Diat, W. Kunz, A. Pfitzner, P. Bauduin, Self-assembly of a short amphiphile in water controlled by superchaotropic Polyoxometalates: H4SiW12O40 vs. H3PW12O40, J. Colloid Interface Sci. 587 (2021) 347–357. https://doi.org/https://doi.org/10.1016/j.jcis.2020.12.003.

[6] N.J. Jain, V.K. Aswal, P.S. Goyal, P. Bahadur, Salt induced micellization and micelle structures of PEO/PPO/PEO block copolymers in aqueous solution, Colloids Surfaces A. 173 (2000) 85–94. https://doi.org/10.1007/s11743-000-0125-0.

[7] P. Taylor, J.B. Hayter, J. Penfold, An analytic structure factor for macroion solutions, Mol. Phys. 42 (1981) 109–118. https://doi.org/10.1080/00268978100100091.

[8] J. Hansen, J.B. Hayter, A rescaled MSA structure factor for dilute charged colloidal dispersions, Mol. Phys. 46 (1982) 651–656. https://doi.org/http://dx.doi.org/10.1080/00268978200101471.

[9] C.D. Dewhurst, I. Grillo, D. Honecker, M. Bonnaud, M. Jacques, C. Amrouni, A. Perillo-Marcone, G. Manzin, R. Cubitt, The small-angle neutron scattering instrument D33 at the Institut Laue – Langevin, J. Appl. Crystallogr. 49 (2016) 1–14. https://doi.org/10.1107/S1600576715021792.